Biol. Cybernetics 35, 81–100 (1979)

Biological Cybernetics

Figure-Ground Discrimination by Relative Movement in the Visual System of the Fly

Part I: Experimental Results

Werner Reichardt and Tomaso Poggio
Max-Planck-Institut für biologische Kybernetik, Tübingen, FRG

Abstract. The visual system of the fly performs various computations on photoreceptor outputs. The detection and measurement of movement is based on simple nonlinear multiplication-like interactions between adjacent pairs and groups of photoreceptors. The position of a small contrasted object against a uniform background is measured, at least in part, by (formally) 1-input nonlinear flicker detectors. A fly can also detect and discriminate a figure that moves relative to a ground texture. This computation of relative movement relies on a more complex algorithm, one which detects discontinuities in the movement field. The experiments described in this paper indicate that the outputs of neighbouring movement detectors interact in a multiplication-like fashion and then in turn inhibit locally the flicker detectors. The following main characteristic properties (partly a direct consequence of the algorithm's structure) have been established experimentally: a) Coherent motion of figure and ground inhibit the position detectors whereas incoherent motion fails to produce inhibition near the edges of the moving figure (provided the textures of figure and ground are similar). b) The movement detectors underlying this particular computation are direction-insensitive at input frequencies (at the photoreceptor level) above 2.3 Hz. They become increasingly direction-sensitive for lower input frequencies. c) At higher input frequencies the fly cannot discriminate an object against a texture oscillating at the same frequency and amplitude at 0° and 180° phase, whereas 90° or 270° phase shift between figure and ground oscillations yields maximum discrimination. d) Under conditions of coherent movement, strong spatial incoherence is detected by the same mechanism. The algorithm underlying the relative movement computation is further discussed as an example of a coherence measuring process, operating on the outputs of an array of movement detectors. Possible neural correlates are also mentioned.

1. Introduction

1.1. The Phenomenon

A small object in front of a textured background usually escapes (monocular) detection and discrimination by a human observer. When the object texture consists of the same (or similar, see Julesz, 1975) structure as the background's texture, monocular discrimination is impossible. If, however, the two textures move relative to each other, the object is easily discriminated against the background. Figure 1 sketches this phenomenon.

Similarly, a fly is able to detect and to discriminate an object that moves relative to a ground texture. A fly usually fixates, i.e. flies towards, a small contrasted object on a white background. Relative movement of a (textured) figure against a textured ground also induces its attempted fixation.

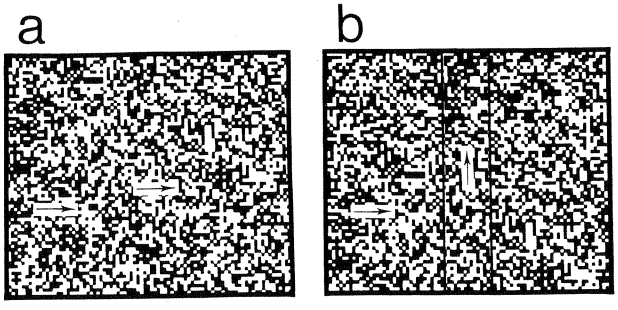

Fig. 1a and b. Random-dot pattern to illustrate the figure-ground separation effect. **a** Figure and ground are both moved horizontally in the same way. The figure, a random-dot textured, vertically oriented stripe, disappears in the ground. The arrows indicate velocity vectors associated with individual contrast elements. **b** If figure and ground are moved relative to each other, the boundary of the figure can be easily detected. The velocity vectors indicate that the ground is moved to the right whereas the figure is moved upward. The black vertical lines represent the perceived boundaries between figure and ground. At these boundaries the velocity vector field is discontinuous. The reader should cut a small stripe out of a random dot texture and verify for herself or him, the effect of relative movement

0340-1200/79/0035/0081/$04.00

In this paper we address the problem of how the fly's visual system accomplishes this detection and discrimination task.

1.2. Visual Control in Flies

The flight behavior of houseflies relies on an elaborate visual control system. A theory developed over the last few years (for a review see Reichardt and Poggio, 1976; Poggio and Reichardt, 1976, 1980) on the basis of experiments pioneered by Reichardt and Wenking (1969), outlines the basic logical organization of one of these control systems, a "smooth" fixation and tracking system. The theoretical description, which is supported by several critical experiments, implies that the fly's visual control of flight relies on two main computations performed on the visual input by thousands of small modules distributed all over the eye. One computation measures movement and the other extracts the position of a visual object, usually by exploiting relative motion with respect to the background.

1.3. The Problem

It is clear that the (angular) position of an object does not exist explicitly in the light inputs to the photoreceptors. Each receptor receives a time-dependent light flux, but does not receive directly position or velocity information. The fly's nervous system extracts both from the image flow. The problem, then, is how do the signals from the photoreceptors interact in order to compute position and velocity? In particular, which algorithm is used by the fly's visual system to discriminate relative movement?

This is the question that we try to answer in this paper. It is a question about the algorithm underlying (in the fly's visual system) the detection and discrimination of an object through relative movement, or in an essentially equivalent way, about the interactions that implement this algorithm. The answer to this question gives one the capability (a) of predicting the system behavior and (b) of building a machine or writing a program that performs these computations in fly fashion.

1.4. Our Approach

It is often difficult to devise an exhaustive list of algorithms performing a given computation and to plan corresponding experiments to check whether these algorithms are actually implemented in a nervous system. For this reason we have developed and used a rather general theoretical approach that amounts to a classification scheme for simple nonlinear algorithms or systems. This theoretical language was critically important for the interpretation and the planning of the experiments described in this paper and it is still necessary for explaining in detail the algorithm underlying the discrimination of relative movement. However, since a satisfactory understanding of this algorithm is available, it is now possible to give a simpler and more transparent account of the experiments and their basic interpretation without direct need of such a theoretical language.

In this first paper (Part I) we give an account of our experiments. In a second paper (Poggio and Reichardt, 1980) we describe the nonlinear system theory we have used. In a third paper (Part II; Bülthoff et al., 1980) we use the theory to characterize the movement and especially the relative movement algorithms, in relation to the experiments described here. We will also describe a computer study showing that the theoretical analysis leads to a number of effective algorithms for relative movement.

We summarize here the organization of this first paper. In Chap. 2 we describe our experimental set-up and methods; we also outline the essence of our theoretical language. Chapter 3 reviews what we know about the algorithms in the fly's visual system that underlie computation of the movement and of position of a small, contrasted object against a white background. We describe the experiments in Chap. 4, together with their interpretation. We also examine some open problems and consider the implications of our findings for more complex cases of figure-ground discrimination. In addition, we discuss our behavioral and "computational" analysis from the point of view of the neural circuitry implementing, in the fly, the detection of relative movement.

2. Experimental Procedures and Methods

In addition to head movements, a fly has, in free flight, six dynamic degrees of freedom: three of translatory and three of rotatory motion. The investigations undertaken so far in our laboratory have been confined to one degree of freedom, either rotation [the rotatory motion of a horizontally flying fly around its vertical axis; Reichardt (1973)] or translation [the vertical motion of a horizontally flying fly; Wehrhahn (1974) and Wehrhahn and Reichardt (1975)]. The measurements were carried out by means of highly sensitive fast mechanoelectric servotransducers, which fix the fly in space and either sense the flight torque or the lift force generated by the wings of a test-fly. When a contrasted optical environment is presented to a fixed flying test-fly, it is operating under "open-loop" conditions. Since the head of the fly is fixed (in all these experiments) to the thorax, a steady pattern represents

a stabilized retinal image for the fly. Contrasted environments were either provided by patterns mounted on cylinders or by electronically generated patterns displayed by oscillographic monitors. In Fig. 2a and b the different techniques used in the experiments are shown in schematic diagrams.

In the figure-ground experiments the figure (either a black or a random-dot, textured, vertically oriented stripe) was oscillated around positions $\pm\psi_0$. In many experiments the ground was also oscillated sinusoidally. Oscillation frequencies covered the range from 0.2 to 8 Hz. Each fly was tested (under open-loop conditions) for 4 min: 2 min with the test figure at position $+\psi_0$ and 2 min at the counter positon $-\psi_0$. The torque response generated by a given fly was averaged by an on-line computer. The responses plotted are: Response average at mean stripe position $+\psi_0$, minus response average at mean stripe position, $-\psi_0$, divided by two. In this way zero biases are elimited from the responses.

Most of the experiments were performed on female, wild type *Musca domestica* from our laboratory stock. Only some experiments were performed on male *Musca*.

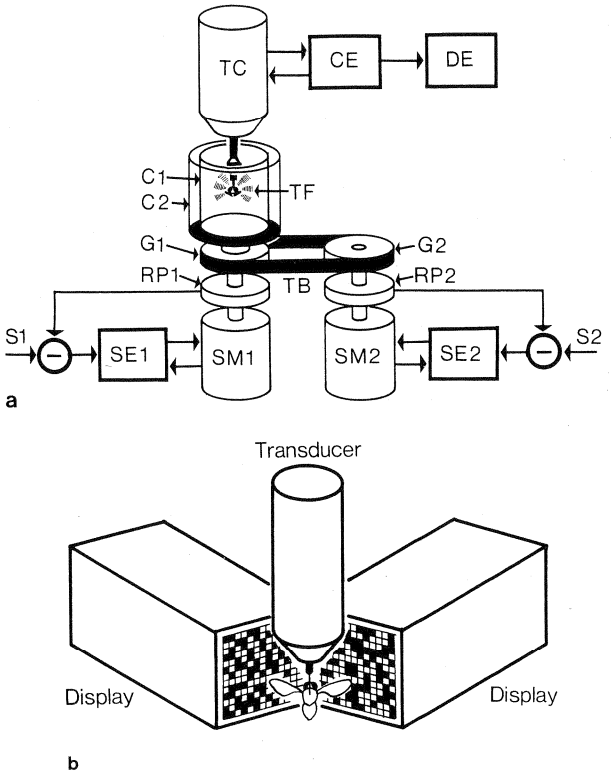

Fig. 2a and b. Schematic representation of the two experimental setups used in the experiments described in this paper. A test-fly TF is suspended from a torque compensator TC which is connected with the compensator electronics CE. The voltage output of CE is proportional to the torque signal generated by the fly under compensation. The CE output is evaluated by the data evaluation box DE. For online data evaluation we used mainly an Intertechnique DIDAC 800 computer. **a** The motion of two cylinders C1 and C2 is controlled by two 400 Hz servomotors SM1 and SM2 whose shafts carry ring potentimeters RP1, RP2 and gears G1 and G2. The inner cylinder is connected with a servomotor SM1 whereas the outer cylinder is driven by a transmission belt TB from servomotor SM2. The ring potentiometer voltages are fed back to the inputs of the servomotor electronics SE1 and SE2, so that SM1 and SM2 are operated under position control from the inputs S1 and S2, respectively. Under these conditions an angular displacement of a cylinder is strictly proportional to the voltage S applied to an input of the SE electronics. The two cylinders are illuminated by four DC current driven fluorescent ring bulbs. The average brightness at the surface of the cylinders amounts to about $700\,cd \times m^{-2}$. **b** The two-cylinder set-up is replaced by two displays (Hewlett-Packard Model 1332 A "white" phosphor) with an average screen brightness of $20\,cd \times m^{-2}$. An electronic device generates a random-dot pattern (figure and ground) with a frame frequency of 244 Hz. In our experiments the figure usually consisted of a rectangular stripe; widths and orientation can be set at will. Figure and ground can be moved independently by a function generator; we mainly used two sinusoidal signals with various phase relations

2.1. *Theoretical Background*

The basic goal is to develop and to use a language that can describe and classify various simple algorithms (and the corresponding systems implementing them). The starting point of the approach chosen here is to consider an algorithm as an operation on an input signal that yields an output. An algorithm can be thought of as an operator, i.e. a rule that associates an output function to each input function. In general, the operators of interest are nonlinear.

The concept of nonlinearity, however, is too general: one has to consider a specific class of nonlinear systems. The important point is that the input-output transductions of interest are "smooth". Heuristically, there seems to be no "decision" or discontinuity involved in the fly's processing of movement and position information. Thus, we restrict ourselves to "smooth", time invariant operators with finite memory. Table 1 shows how these "smooth" systems can be decomposed in a standard way, as the sum of simpler, canonical systems. In this fashion, a many input nonlinear system is represented as the sum of linear systems, quadratic (i.e. multiplication-like) systems and so on. The representation is essentially a kind of Taylor series development for systems (instead of functions). A multi-input linear system has only the first type of graphs in Table 1b (linear graphs). The second type of graph represents a multiplication-like interaction between the same input (see c) or between two distinct inputs (see d). This multiplication-like interaction is precisely defined in Table 1d. The structure of higher order terms can be easily inferred.

In this way we have a canonical representation and classification scheme for a large class of "smooth" nonlinear systems. As shown by Poggio and Reichardt

Table 1. A large class of multi-input systems can be decomposed into the sum of simpler systems, denoted by appropriate graphs (a). Each graph (b)–(d) is a shorthand notation for an explicit mathematical representation. The power series development of a system, presented in (e), is a generalisation of the well known Taylor development of a function

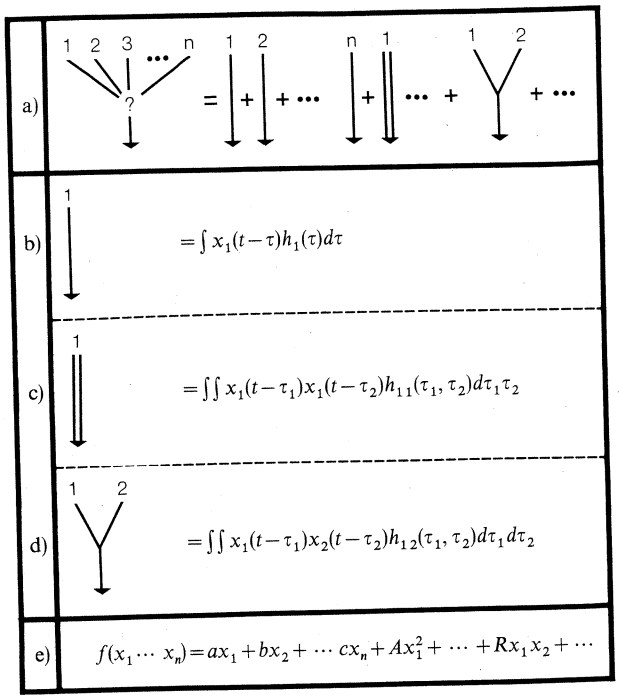

Table 2. Classification of graphs for movement detection

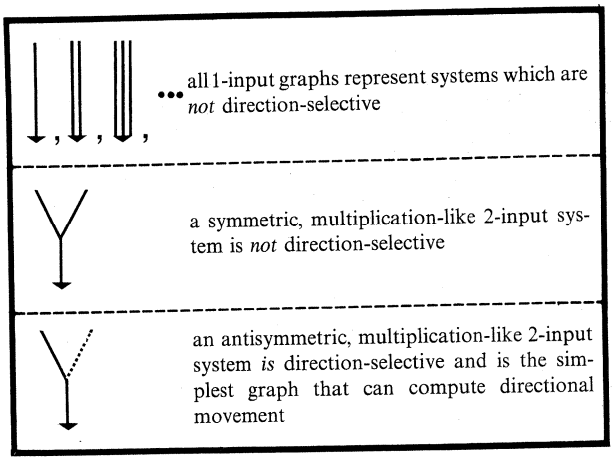

(1980), specific information processing properties can be associated with each graph. In addition, it is also possible to characterize rather exhaustively the functional properties of any term. Thus, for any given computation say for instance the computation of directional movement, we can state which graphs (and combinations thereof) can implement it. This corresponds to a classification of the algorithms for the particular computation. The next step then is to devise experiments that can tell which of the algorithms (or graphs) are actually used by the fly's visual system.

As we have already mentioned, we present in this paper a more intuitive approach, rather independent from this theoretical language. Part II will deal with the fly's computation of movement and relative movement from a theoretical point of view (see also the recent overview by Poggio and Reichardt, 1980).

3. Movement and Position Computations

3.1. Movement

Table 2 defines what we understand by computation of directional motion and also indicates which of the simpler terms in our canonical representation can perform it. It is clear that for the computation of directional movement, signals from at least two photoreceptors must be compared. Moreover, if we require that the time averaged output is direction-selective, the interaction between the two inputs must be nonlinear, since the average output of a linear system is a linear combination of the input's averages. That movement detection must rely on nonlinear interactions is also clear, because detection of movement is equivalent to the detection of phase-difference between two inputs and this is a nonlinear operation. The simplest operation that can perform movement detection is thus a multiplication-like interaction between two inputs (from two photoreceptors or two groups of photoreceptors). The interaction must be asymmetric, in the sense that the two channels are not equivalent, since otherwise the output would not be different for different directions of motion. The simplest model of this type is in fact a pure multiplication of the two signals, after delaying (or low-pass filtering) one of the two (see Fig. 3). It is now well established that the computation of directional movement is carried out in the fly's and other insect's visual systems through such an algorithm, proposed first by Hassenstein and Reichardt[1].

If the output of a movement detector is completely antisymmetric (i.e. the two directions of motion give equivalent outputs, modulus the sign), the overall corresponding interaction is also antisymmetric (see Table 2). It is clearly always possible to synthesize an antisymmetric interaction from an asymmetric one, as shown in Fig. 3b, which represents a version of the original model proposed by Reichardt and

1 Hassenstein (1951, 1958, 1959), Hassenstein and Reichardt (1956), Reichardt (1957, 1961, 1969, 1970), Reichardt and Varjú (1959), Varjú (1959), Fermi and Reichardt (1963), Götz (1964, 1972), McCann and MacGinitie (1965), Thorson (1966a, b), Hengstenberg and Götz (1976), Varjú and Reichardt (1967), Eckert (1973), Marmarelis and McCann (1973), Poggio and Reichardt (1973a, b), Buchner (1974), Pick (1974a, b, 1976), Poggio (1974), Pick and Buchner (1979)

Hassenstein. As will be seen later, the interaction underlying movement is likely to be the basic element for the detection of relative movement.

3.2. *Position*

Table 3 gives a definition of this computation, that is detection of a contrasted small object. The output of the computation is required to drive an eye centering servomechanism. Thus, the sign of the output must depend on whether the image of the target is in the right or left eye. It is clear that an array of modules distributed in the eye, each receiving input from an individual photoreceptor, *can* perform this computation. Each graph (in our terminology) has a "weight" or an amplification factor parametrized by its position in the eye (see Fig. 4). These modules could operate in a linear fashion. In order, however, that stabilized retinal images give a zero average output such 1-input graphs (or modules) must be nonlinear, for instance of degree two (see Table 3). The simple 1-input algorithm seems to underly position computation in the fly. The experiment, which shows that more complex interactions are not *necessary* is due to Pick (1974a). For small contrasted objects against a uniform background (less than 6° in angular extent on the horizontal plane) 1-input "flicker" detectors, distributed everywhere in the eye, certainly play a role in this computation. However, some caution is needed before concluding that *only* 1-input detectors are active; transient responses, certainly important in free flight behavior, may also be based on detectors with two or more inputs. Such detectors may be relatively unresponsive to flicker and may require transiently moving stimuli. As we will discuss in Part II, 1-input flicker detectors are generated within the Volterra formalism by almost all physiological movement detectors.

4. Relative Movement Detection

4.1. *Basic Properties*

In the introduction we stated that flies can detect a small object against a textured background, provided there is relative motion between "figure" and "ground". The first demonstration of this phenomenon was given by Virsik and Reichardt (1974, 1976) in a series of closed-loop experiments. Under this condition, a fly suspended by the torque compensator controls by its torque signal, processed by a simulator of the flight dynamics, the angular velocity of a ground texture and of an object in front of it. If there is even a small relative motion between the two, the fly fixates and tracks the target. Open-loop experiments, in which the fly does not control the motion of its visual environment, demonstrate the same effect

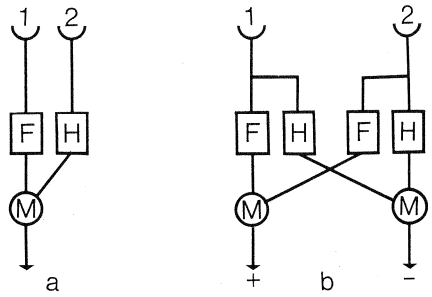

Fig. 3. a A part of the model of movement detection of Hassenstein and Reichardt (1956). The two inputs are multiplied after low pass filtering with different time constants. If an average operation is made on the output the overall operation is equivalent to a crosscorrelation of the two inputs. **b** The output of this and its complementary scheme represents the behavioural optomotor response of the whole insect. While the interaction between input 1 and 2 is asymmetric in **a**, the scheme shown in **b** is antisymmetric: reversal of the direction of motion simply reverses the sign of the output

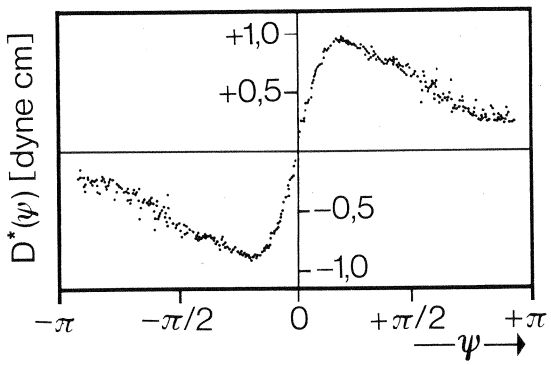

Fig. 4. The "weight" or amplification factor $D(\psi)$ parametrized by its angular position ψ, where ψ designates the angular position of the image of an object (stripe) on the retina of the two compound eyes in a horizontal plane. $\psi = 0$ refers to the symmetry-line between the two eyes. Redrawn from Reichardt (1973)

Table 3. Classification of graphs for position detection

↓	an array of such (weighted) graphs *can* perform the position computation. Stabilized images are "seen".
⇓	an array of such (weighted) graphs *can* perform the position computation. Stabilized images may not be seen.
Y	*cannot* perform the computation

(Heimburger et al., 1976). The flicker detectors, discussed earlier and sketched in Table 3, can of course detect a small contrasted object moving against a stationary ground, but they are clearly helpless if the ground also moves relative to the eye. In this case flicker detectors are stimulated all over the eyes and not only in the position where the image is located.

In Part II we give a classification of the algorithms capable of implementing relative movement detection and discrimination. The basic points, however, are rather easy to see. If relative motion is evaluated, all flicker detectors in the eye have to be inhibited (at least in part) except the ones near the discontinuities in the velocity field, because velocity discontinuities imply, in the standard hypothesis of object rigidity, that a different object is there. Thus, in addition to the 1-input flicker detectors, this computation receives a center-surround organization of directionally selective movement detectors which inhibit the flicker detectors when there is the same movement in the center as in the periphery. The rigorous analysis of Part II shows that the interaction of direction-insensitive movement detectors or even of flicker detectors can play a similar role, although with different efficiencies, as shown by the computer experiments. Table 4 summarizes these conclusions and shows some of the simplest algorithms that can implement relative movement detection. Table 5 shows how the average output of the various graphs (or algorithms) depends on the phase between small amplitude, sinusoidal oscillations (same frequency) of figure and ground. These results, derived in Part II, are valid for the ensemble average of several such graphs or modules in different positions (in the eye) with respect to the patterns. In Table 5a the first possibility is depicted, the interaction of two direction-sensitive movement detectors. It is clear that inhibition (of the flicker detectors responding to the object) will be maximum when movement is the same in the center and in the surround. When the phase shift is 180°, the inhibition is turned into excitation. The algorithm of Table 5b, on the other hand, is based on direction-insensitive movement detectors. Since direction of movement is not important, 0° and 180° phase shifts are equivalent in providing maximum inhibition! The same obtains for the graph of Table 5c, based on flicker detectors. In Table 5d a more complex possibility is depicted. The two pairs of inputs are intrinsically different, one being able to respond only to large field

Table 4. Classification of graphs for the detection of relative movement

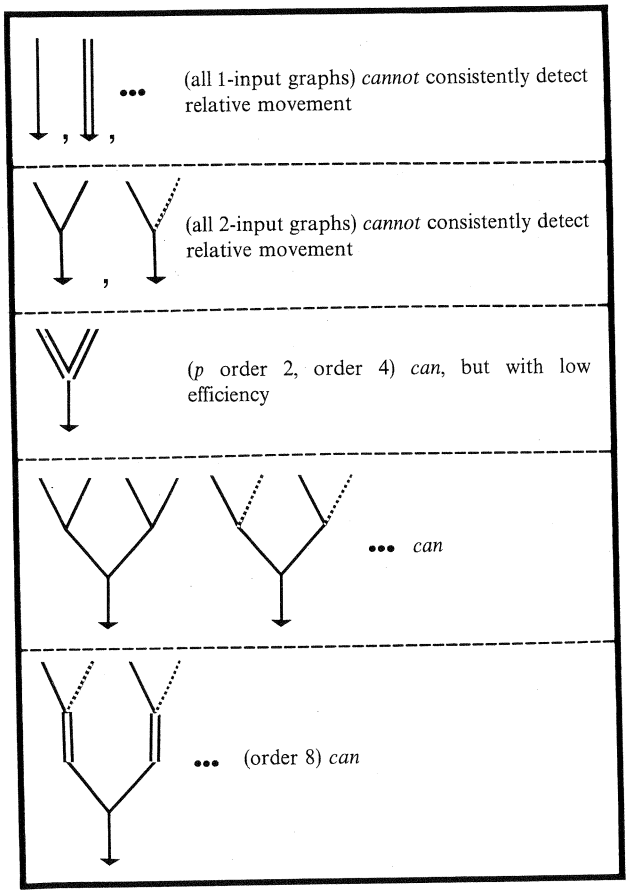

Table 5. Properties of some graphs for sinusoidal oscillation of figure against ground

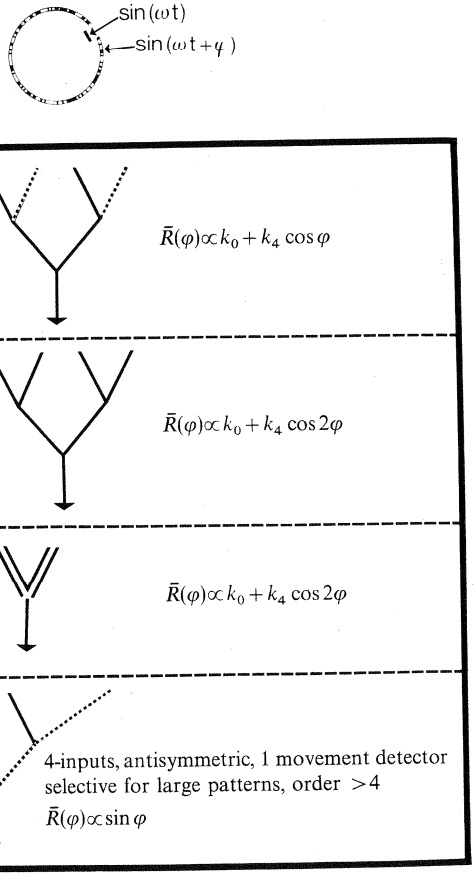

movements, i.e. in this case to the ground texture. As a consequence, the response may contain $\sin\varphi$ components.

Let us now turn to our main question: which algorithms for relative movement detection and discrimination are implemented by the visual system of the fly? Later we will analyze various properties of the fly's computations in more detail.

4.2. *Experimental Results*

First, we briefly outline the experimental procedure (see inset of Fig. 5). The (flying) fly is fixed in space and its torque around the vertical axis is measured. Positive (negative) torque means that the fly tries to turn to the right (left).

A black object (a small, vertically oriented stripe) is sinusoidally oscillated at 2.5 Hz around a fixed position ($\psi_0 = \pm 30°$) in front of one of the two compound eyes. A random-dot textured ground is also oscillated with the same frequency and a relative phase φ (relative to the oscillated object). The average attraction of the fly by the object, defined as the time average of the fly's torque response, is measured in units of the standard response to the object oscillating in front of the stationary ground texture (the amplitude amounts to $\pm 0.5°$ for the ground and to $\pm 1.0°$ for the object). Figure 5 shows that the strength of the discrimination is reduced when the phase is either $\varphi = 0°$ or (surprisingly!) $\varphi = 180°$. Under the condition $\varphi = 0°$ the two movements are "coherent", whereas under the $\varphi = 180°$ condition the two movements are in opposite phase. The attraction of the fly by the object reaches its maximum for $\varphi = 90°$ and is also strong when object and ground oscillate with different frequencies. An opaque white screen (12° wide), interposed between the object and the ground, as shown in the inset of Fig. 5, does not have any influence on the effect. This observation indicates the existence of lateral (nonlinear) interactions between the signals from receptors stimulated by the object and the signals from receptors stimulated by the ground. The phase portrait is, on the whole, well approximated at this oscillation frequency by

$$\bar{R} = k_0 + k_4 \cos 2\varphi \qquad (1)$$

which speaks in favour of algorithms (b) and (c) in Table 5. Before considering further which one of these two possibilities is actually realized in the fly's visual system, let us consider the effect in more detail. Another version of the experiment is shown in Fig. 6. In this experiment object and ground are again oscillated with equal frequencies, but with equal amplitudes ($\pm 1°$). It can be seen from the phase dependence of the averaged response, plotted in Fig. 6, that the object is

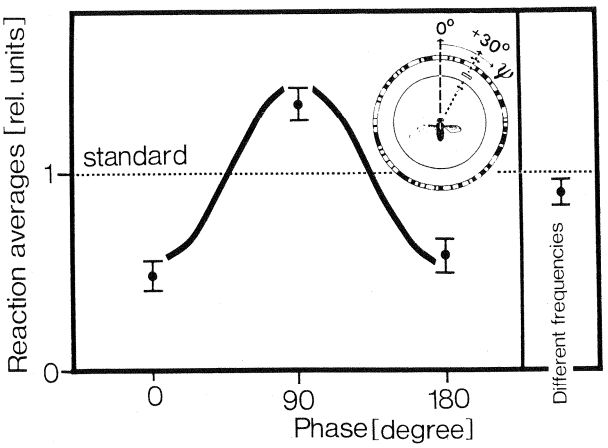

Fig. 5. Phase dependence of the figure-ground discrimination effect. Average torque responses of ten flies to sinusoidally oscillating figure and ground patterns, measured in the equipment shown in Fig. 2a. The figure consists of a black, vertically oriented stripe, 3° wide, positioned in the lower part of the panorama, oscillated around the mean positions $\psi_0 = \pm 30°$. The ground pattern consists of a random-dot texture which can be moved independently from the stripe. A white stationary screen (12° wide) is mounted between the stripe and the ground pattern in order to avoid mixed stimulations of receptors by the stripe and by the ground. In all experiments shown in the figure, the oscillation amplitude of the stripe amounted to $\pm 1°$ (at 2.5 Hz frequency) and $\pm 0.5°$ for the random-dot textured ground (when oscillating). The standard response (dotted horizontal line) measures the attraction of the fly by the stripe when oscillated alone, while the ground was stationary. When stripe and ground are both oscillated with the same frequency, the average attraction towards the stripe depends on the relative phase, as shown in the left side of the figure. When stripe and ground are oscillated with different frequencies (2.5 and 1.8 Hz, respectively), the average attraction is about "standard". Each point is the mean of ten individual measurements. Each individual measurement lasted 2 min, so that each response, measured at 2.5 Hz, is the average of 300 cycles and at 1.8 Hz of 216 cycles. The vertical bars denote standard errors of the mean. The continuous line is drawn by (hand) fitting the experimental data with Eq. (1), where k_0 is determined by the "standard" response ($k_0 = 1$) wherease k_4 is the free parameter. Redrawn from Poggio and Reichardt (1976)

not discriminated for phases $\varphi = 0°$ and $\varphi = 180°$ whereas the discrimination is best at about $\varphi = 90°$ and $\varphi = 270°$. Essentially the same result is obtained when the black stripe is replaced by a stripe 10° wide, consisting of the same random texture as the ground (see Fig. 7). Figure and ground were oscillated with equal frequencies (2.5 Hz) and equal amplitudes ($\pm 5°$). The response is smaller (compare Fig. 6), because this experiment was carried out at a much lower average brightness characteristic of the display tubes shown in Fig. 2b.

In the experiment represented in Fig. 7, the random-dot textured figure moved relative to the ground without any screen in between. If the object consists of a random texture moving behind a window, so that no moving edges are present, the effect remains unchanged, indicating that the moving edges of the

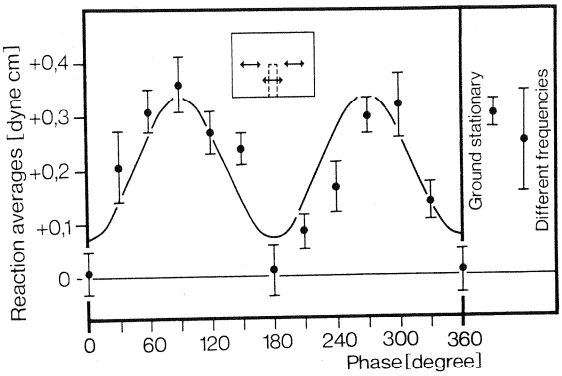

Fig. 6. Phase dependence of the figure-ground discrimination effect. Experimental conditions as described in the legend and in the inset of Fig. 5, except for equal oscillation amplitudes of $\pm 1°$ for the stripe and the random-dot textured ground. The two points on the right side of the figure are response averages taken when stripe and ground oscillated with different frequencies and when the stripe oscillated and the ground was kept stationary. Each point in the figure represents the average from 10 flies. The responses are plotted in absolute units. The vertical bars denote standard errors of the mean. The continuous line is the component $k_4 \cos 2\varphi$ in Eq. (1), derived from a Fourier analysis of the data plotted in the figure. The inset of the figure indicates the stimulus conditions. Redrawn from Reichardt (1978)

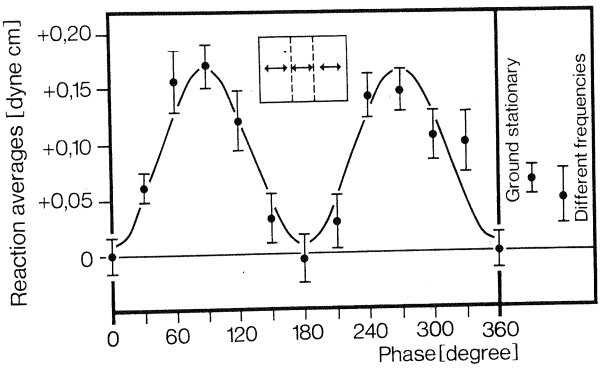

Fig. 7. Phase dependence of the figure-ground discrimination effect. The experimental conditions are as described in the legends of Figs. 5 and 6 except that figure and ground consist of the same random-dot textures, generated on two displays, as described earlier in Fig. 2b. The figure is a vertically oriented random-dot textured stripe of 10° width. Figure and ground were moved horizontally with equal amplitudes of $\pm 5°$. The average position of the figure on the eye was $\psi_0 = \pm 30°$. There are no "screens" interposed between figure and ground. The left side of the plot contains the phase dependence of the averaged responses, whereas the right side represents the averaged reactions to the oscillating figure (stationary ground) and to the oscillating figure and ground for nearby incommensurate frequencies: 2.5 Hz for the figure and 1.8 Hz for the ground. Each point is the average from 10 flies. The responses are plotted in absolute units. The vertical bars denote standard errors of the mean. The continuous line is the component $k_4 \cos 2\varphi$ in Eq. (1), derived from a Fourier-analysis of the data plotted in the figure. Redrawn from Reichardt (1978)

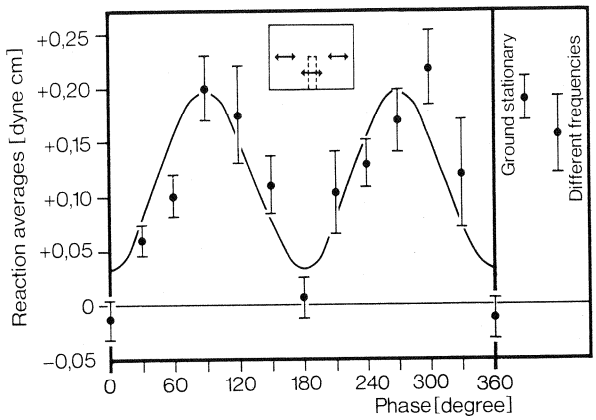

Fig. 8. Phase dependence of the figure-ground discrimination effect. Experimental conditions as described in the legend and in the inset of Fig. 6 apart that the 3° wide stripe, in front of a 12° wide, stationary white screen, was oscillated around the mean positions $\psi_0 = \pm 60°$. In comparison to Fig. 6, the responses are weaker but show the same characteristic phase dependence

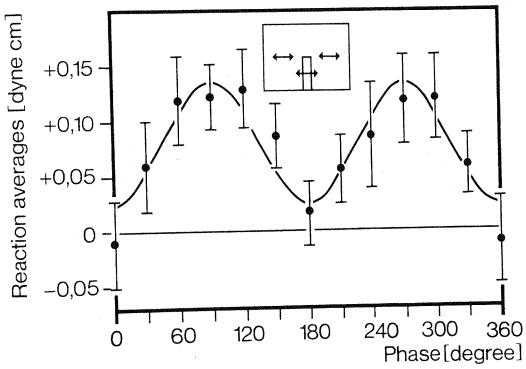

Fig. 9. Phase dependence of the figure-ground discrimination effect. Experimental conditions as described in the legend and in the inset of Fig. 6. The 3° wide stripe, in front of a 12° wide, stationary screen, was oscillated around the mean positions $\psi_0 = \pm 90°$. In comparison to Figs. 6 and 8, the responses are weaker and the errors of the mean are larger but the characteristic phase dependence seems to be unchanged

figure are not the primary source for figure-ground separation.

These results do not depend on the location of the figure on the compound eye. This is shown in Figs. 8 and 9 where the experiments described in Fig. 6 were repeated at the positions of $\psi_0 = \pm 60°$ and $\psi_0 = \pm 90°$ respectively. Especially for $\psi_0 = \pm 90°$ the scatter in the data is larger and the size of the average response is half the response obtained at $\psi_0 = \pm 30°$. These results lead to the conclusion that the interactions mediating figure-ground separation are not restricted to frontal parts of compound eyes.

Finally, the dynamics of the response is shown in Fig. 10 for various relative phases between the object (the reference) and the ground texture. The direction-

sensitive optomotor reaction, which closely follows the motion of the ground, dominates, thus leading to a strong first harmonic in the response. The figure-ground discrimination effect is evident in the average response level.

In summary, the most surprising outcome of the experiments presented so far is the observation that figure-ground discrimination disappears under the condition of antiphase oscillation, that is when the phase shift between the figure and the ground amounts to $\varphi = 180°$. This supports the types of interaction shown in Table 5b and c, at this oscillation frequency. There is good agreement of the phase dependent response with Eq. (1); the continuous lines in Figs. 6–9 are derived from a Fourier analysis of the data plotted in the figures. They represent the second harmonic present in the data, that is the term $\cos 2\psi$ of Eq. (1).

4.2.1. Interplay between Inhibition and Excitation. Even in terms of the highly simplified analysis outlined in this paper, one expects that an increased amplitude of the oscillating figure should lead to an increase of the contributions from the excitatory local self-interactions which are stimulated by the oscillating figure. Figure 11 shows that this is indeed the case. A small object is oscillated in front of a random textured ground with an amplitude ($\pm 5°$) five times the amplitude ($\pm 1°$) of the oscillating ground. The test-flies are attracted by the object even at phase angles 0° and 180°. The attraction of the fly reaches its maximum at $\varphi = 90°$ and $\varphi = 270°$, quite in accordance with Eq. (1) where now $|k_0| > |k_4|$. The continuous line in Fig. 11 is the second harmonic computed by a Fourier analysis of the data.

The opposite situation ($|k_0| < |k_4|$) may occur when the oscillation amplitude of the ground is increased and the oscillation amplitude of the figure remains fixed, since under these conditions the effect of lateral inhibition may be larger. The outcome of a sequence of such experiments is shown in Fig. 12. For $\varphi = 0°$ and $\varphi = 180°$, the attraction of the object disappears (for equal amplitudes of object and ground). For increasing ground amplitudes the inhibition overrides the excitatory contributions of the self-interactions: The fly tries to escape from the object. For $\varphi = 90°$ the inhibition turns into excitation and the attraction of the fly by the stripe increases. A number of factors reduce the effect at large amplitudes, especially the increasingly high speed of the ground together with the appearance of higher harmonics in the inputs to the photoreceptors.

So far we have discussed the interplay between signals elicited by the figure and by the ground. An interesting question concerns the conditions under which the influence of the figure on the response becomes independent of the effect of the ground texture, since only under this condition can perfect figure-ground discrimination be claimed. From the schemes of Table 5 it is clear that, for random textures, the inhibition term should disappear (in the average

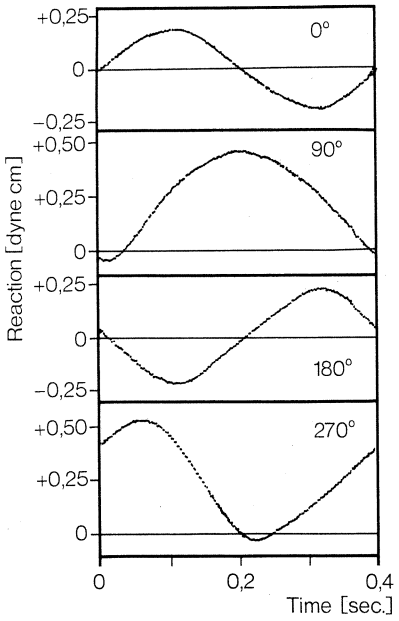

Fig. 10. The fly's instantaneous response in a typical figure-ground experiment, as described in Fig. 6. The experimental parameter is the relative phase between the oscillating figure and the oscillating ground. Under 0° and 180° phase conditions, the test-fly responds sinusoidally; the average reaction is zero, quite in accordance with the result reported in Fig. 6. The sinusoidal response reflects the contributions from the antisymmetric optomotor reaction graphs. At 90° and 270° phase shifts between figure and ground, higher harmonics (mainly the second harmonic which amounts to about 15% of the first harmonic) appear and the average response is greater than zero, in accordance with the two maxima in Fig. 6. The oscillation frequency amounted to 2.5 Hz and the oscillation amplitude to $\pm 1°$

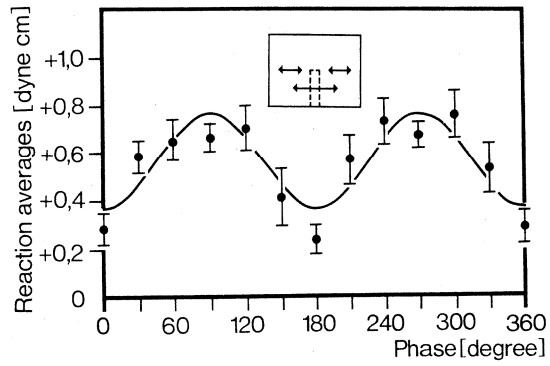

Fig. 11. Phase dependence of the figure-ground discrimination effect. Experimental conditions as described in the legend of Fig. 6, except for different oscillation amplitudes $\pm 1°$ for the ground and $\pm 5°$ for the stripe). Note that the fly is attracted by the oscillating stripe (3° wide) even at phases $\varphi = 0°$ and $\varphi = 180°$

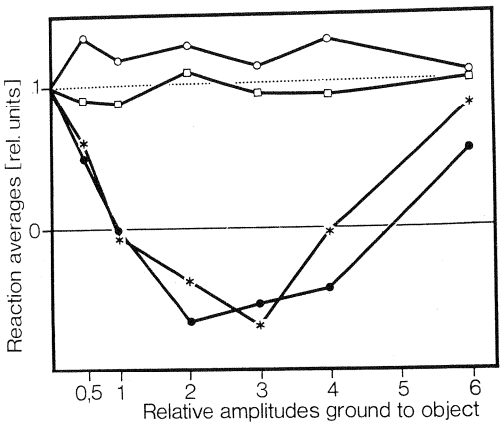

Fig. 12. Experimental details as described in the legends of Figs. 5 and 6, except for different oscillation amplitudes of the ground with respect to the stripe's oscillation amplitude of $\pm 1°$. The relative phase relations between stripe and ground are: 0° (●●●), 90° (○○○), 180° (***). □□□ designate measurements with different frequencies (2.5 Hz for the stripe and 1.8 Hz for the random-dot textured ground). The average standard errors of the mean amount to ± 0.1 relative units. From Poggio and Reichardt (1976)

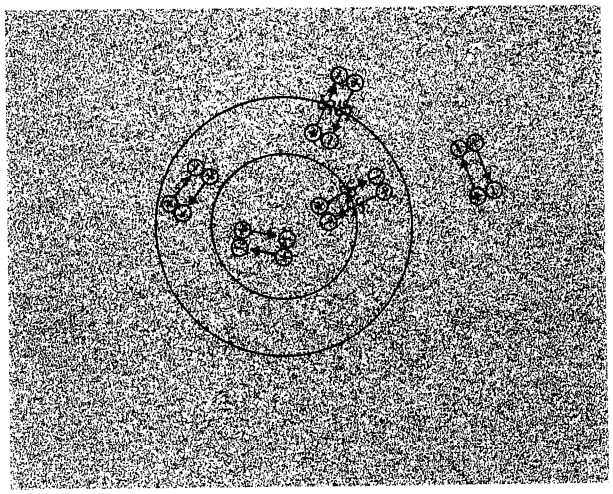

Fig. 13. An illustrative outline of the figure-ground discrimination effect through relative movement. Figure (ring) and ground consists of the same random-dot texture. Without relative motion between figure and ground, the figure "disappears" in the textured ground. When ring and ground are moved relative to each other, the boundaries of the ring become easily visible. When a fly is flying relative to the pattern shown here, each contrast element contributes with an "excitatory" (attraction) component, designated with (+). The signals received at the photoreceptor level are motion coherent if they originate from texture elements which are not moving relative to each other. They induce inhibitory contributions (−) which compensate the excitatory (+) ones. However, coherency breaks down and consequently inhibition (−) disappears across the two boundaries of the ring whenever the figure (ring) is moved relative to the ground. This effect is indicated by the double wavy lines SS. When a figure is discriminated from a ground the part of the nerve net receiving stimulation from the figure becomes independent of the influence of the part receiving stimulations from the ground. From Reichardt (1978)

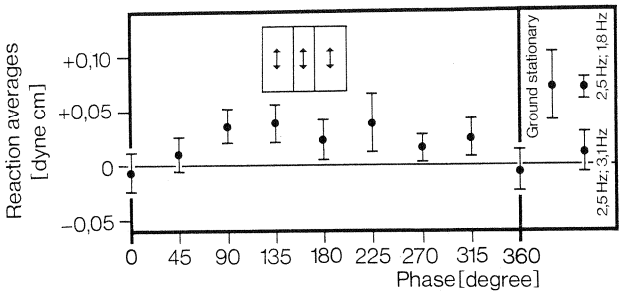

Fig. 14. Phase dependence of the figure-ground discrimination effect. Experimental conditions as described in the legend of Fig. 7, except that figure and ground are oscillated vertically. The right side of the figure contains averaged responses to the oscillating figure with the ground kept stationary, and to figure and ground oscillating with different frequencies. The figure was always oscillated at 2.5 Hz. Each point represents the average from 10 flies. The vertical bars denote standard errors of the mean. Redrawn from Reichardt (1978)

response) when ground and figure motions are incoherent. This condition is fulfilled when different oscillation frequencies f_1 and f_2 (nearly incommensurate) are used in the experiments. The results from two sets of experiments with stationary ground and with two different oscillation frequencies for the figure and the ground are also plotted in Figs. 6–8 and 12. The reaction averages are not significantly different from each other.

This result can be visualized in Fig. 13. The figure here consists of a ring whose texture is the same as the ground's. If figure and ground are not moved relative to each other the ring "gestalt" disappears in the ground and it remains hidden when figure and ground are moved together relative to the eyes. However, as soon as the figure moves relative to the ground, for instance with different oscillation frequencies, the (mean) inhibitory contributions across, and only across, the boundaries of the figure disappear. This imbalance of inhibition and excitation determines (in the fly) a turning signal towards the figure. In a sense the modules receiving optical stimulation from the figure become independent from the ground.

4.2.2. Characterizing the Algorithm. The experimental results reported so far are in acordance with both interaction schemes of Table 5b and c. Let us now consider the question of whether the algorithm used by the fly's visual system relies on 2 or 4 inputs. Clearly, in the case (c) of a symmetric interaction between flicker detectors, the response must be independent of the orientations at which figure and ground are moved relative to the fly's eye. This need not be the case for the algorithm (b), since here individual movement detectors, although direction-insensitive, are oriented. Figure 14 shows the result of an experiment where the figure (a textured stripe) and the ground were moved

vertically. Comparison between the experiments of Fig. 7, carried out under identical conditions, leads to the conclusion that the algorithm implemented by the fly (at this oscillation frequency) cannot rely on the interaction between flicker detectors (Fig. 5c) and corresponds instead to the interaction between pairs of direction-insensitive movement detectors (Table 5b). The effect shown by the experiment of Fig. 14 must depend on the interaction of two movement detectors with a horizontal orientation (or at least a horizontal component). The experiment of Fig. 14 excludes the presence of significant interactions between vertically oriented movement detectors.

The two sets of experiments, however, do not contain information about possible cross-interactions between input pairs of different orientations. In order to determine whether such interactions are realized, we have performed two sets of figure-ground experiments in which the ground was oscillated horizontally and the figure was oscillated vertically.

The experiments were performed in two different ways:

a) The phase condition $\varphi = 0°$ is defined as follows: When the figure is presented to the right eye and the ground moves from front to back (on the eye), the figure moves upward. When the figure is presented to the left eye and the ground moves from front to back, the figure moves upward.

b) The condition $\varphi = 0°$ is now defined by the following convention: When the figure is presented to the right eye and the ground moves from front to back, the figure moves upward. When the figure is presented to the left eye and the ground moves from back to front, the figure moves upward.

Experiments under condition a) provide us with information over the entire phase range from $\varphi = 0°$ to $\varphi = 360°$, whereas under condition b) the phase range $\varphi = 180°$ to $\varphi = 360°$ must mirror the measurements taken in the range $\varphi = 0°$ to $\varphi = 180°$, under the assumption of functional symmetry between the two compound eyes, since the data are the difference between the responses with the figure on the right eye and with the figure on the left eye. The two sets of experiments are not independent; once the responses are measured under condition a) they can be predicted under condition b), if the two eyes are symmetric. Figure 15 refers to the data measured in condition a) and Fig. 16 to the data measured in condition b). A comparison of Figs. 15 and 16 shows that the two sets of reactions are not significantly different, confirming that the two eyes are functionally equivalent. Moreover, the response sizes at phase angles $\varphi = 90°$ and $\varphi = 180°$ are in the same order as in Fig. 7, suggesting that there are cross-interactions between horizontally (ground) and vertically (figure) oriented

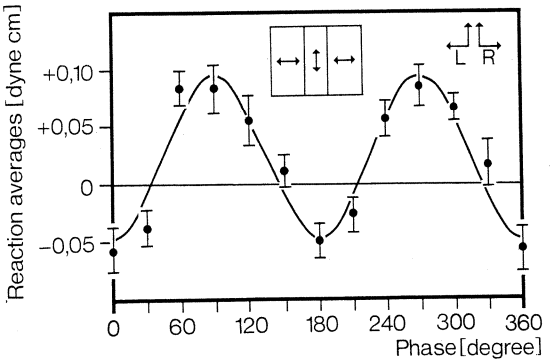

Fig. 15. Phase dependence of the figure-ground discrimination effect. Experimental conditions as described in the legend of Fig. 7. The random-dot textured figure was oscillated vertically whereas the random-dotted ground oscillated horizontally (see inset in the central upper part). We define the phase 0° between figure and ground oscillations with the following convention (valid for the right eye): when the ground moves to the right, the figure moves upward. The complementary situation is applied for stimulations of the left eye. The two conditions are indicated by the inset in the upper right part of the figure. Under these experimental conditions every phase φ leads to an independent response. Each point represents the average from 10 flies. The vertical bars denote the standard errors of the mean. Note that the reactions are slightly negative at phases $\varphi = 0°$ and $\varphi = 180°$

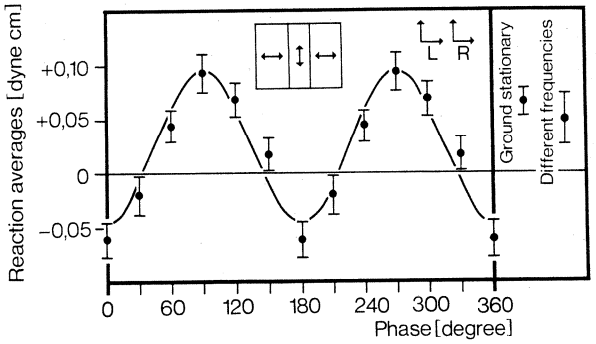

Fig. 16. Phase dependence of the figure-ground discrimination effect. Experimental conditions as described in the legend of Fig. 15. Right and left eye, however, are not symmetrically stimulated. That is, for $\varphi = 0°$, the figure moves upward when the ground moves to the right. This condition is indicated by the inset in the upper right part of the figure. The stimulus conditions repeat after 180° phase shift. Consequently, measurements taken in the phase region $0° \leqq \varphi \leqq 180°$ were averaged with the corresponding measurement in the region $180° < \varphi < 360°$. Each point is therefore an average from 20 individual flies. The vertical bars, indicating the errors of the means, are smaller than in Fig. 15. On the right side two additional measurements are plotted: the mean response to the oscillating figure when the ground was at rest and the response to the oscillating figure and ground when oscillated with different frequencies (2.5 Hz for the figure and 1.8 Hz for the ground). Redrawn from Reichardt (1978)

pairs of inputs. In a complementary experiment the ground was moved vertically and the figure was moved horizontally (Fig. 17). There is again a clear and consistent phase-dependent response, suggesting again that cross-interactions between pairs of horizontally

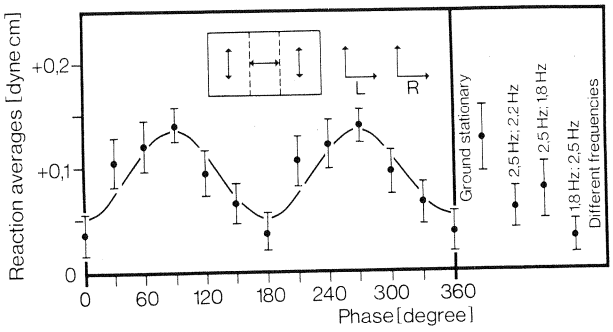

Fig. 17. Phase dependence of figure-ground discrimination. Experimental conditions as described in the legend of Fig. 15. However, the figure oscillated horizontally whereas the ground oscillated vertically (see inset in the upper part). The relative phase between figure and ground oscillations is defined for $\varphi = 0°$: when the figure moves from left to right, the ground moves upward. Right and left eye are stimulated under identical phase conditions, again not symmetrical. The stimulus conditions repeat after 180° relative phase shift. Therefore, measurements taken in the phase region $0° \leqq \varphi \leqq 180°$ were averaged with corresponding measurements in the region $180° < \varphi < 360°$. Each point is an average from 20 individual flies. The vertical bars denote the error of the mean. On the right side four additional measurements are presented: the mean response to the oscillating figure when the ground was kept at rest and the response to the oscillation of figure and ground when moved with different frequencies (1.8 or 2.5 Hz for the figure, 1.8, 2.2, and 3.1 Hz for the ground)

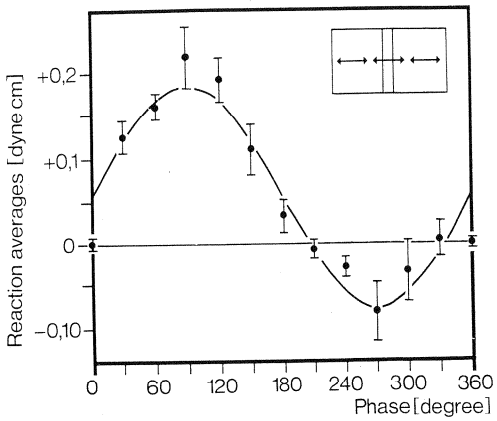

Fig. 18. Phase dependence of a figure-ground discrimination experiment. The experimental conditions are the same as described in the legend for Fig. 5, except for the following conditions: the figure is a 6° wide random-dot texture, figure and ground are oscillated with an amplitude of ±3°; oscillation frequency of figure and ground amounts to 0.5 Hz. Note the dramatic change in the phase portrait (especially in the region between 180° and 360° relative phase). Other experiments have shown that this change is entirely due to the low oscillation frequency. Each point is an average from 10 individual flies. The vertical bars denote the error of the mean

Table 6. Orientations of input-pairs, responsible for figure-ground discrimination and cross-interaction between these pairs

Orientation of the inputs stimulated by the ground	Interaction between pairs of inputs	Orientation of the inputs stimulated by the figure
—	YES	—
|	YES	—
—	YES	|
|	NO	|

(figure) and vertically (ground) oriented inputs exist. In addition, the different form of the response suggests that the vertically and horizontally oriented movement detectors may have a different specificity to large and small field movements. Later we will discuss other experiments that require a similar property.

In summary then, the outcome of the experiments, reported in Figs. 7 and 14–17 lead to the conclusion that the elementary computational structure responsible for figure-ground discrimination consists of four inputs (Table 5b). There are vertically and horizontally oriented pairs of direction-insensitive movement detectors. Interactions exist in three combinations as shown in Table 6.

4.2.3. The Algorithm at Different Oscillation Frequencies. The figure-ground phase-experiments, described so far, have been carried out with an oscillation frequency of 2.5 Hz, with various amplitudes, in various regions of the eye and with various figure and ground textures. In a series of additional experiments we have also tested whether and how the phase-portrait depends on the frequency of oscillation. If one increases the frequency (up to 8 Hz) of figure and ground, the picture does not change, except that the response is scaled down. However, oscillation frequencies below 1.5 Hz lead to a dramatic change which settles at about 0.5 Hz. The response contains then a strong $\sin\varphi$ component and can be approximated by

$$\bar{R} = k_0 + k_4 \sin\varphi \qquad (2)$$

with $k_0 > 0$ and $k_4 > 0$. At even lower frequencies (down to 0.2 Hz) this dependency does not change, except for a factor which diminishes the strength of the time averaged response. An experiment carried out at an oscillation frequency of 0.5 Hz is shown in Fig. 18. In this lower frequency range the algorithm used by the fly looks like the graph in Table 5d, that is the antisymmetric interaction of two directional-sensitive movement detectors. The two movement detectors are not equivalent: one must respond only to the background motion, being for instance a large field

detector, which may be synthesized from the sum over large regions of the eye of small field detectors, followed by a threshold mechanism. The higher harmonics present in the plot of Fig. 18 can be accounted for by the presence of such a threshold mechanism (see Part II). Graph (d) requires 4 inputs, as does graph (b), which underlies the higher frequency effect. This is consistent with the idea that the two graphs may originate from the same mechanism. As a matter of fact, simple models can be devised: for instance the interaction of two asymmetric movement detectors, where the antisymmetric filter property disappears with increasing oscillation frequency, is equivalent to graph (d) in the limit of low frequencies and to graph (b) in the limit of high frequencies. This hypothesis seems to account for the complex change of the harmonic content of the phase portraits with oscillation frequency (see Part II).

In conclusion, the algorithm used by the fly's visual system to detect relative movement is based on a multiplication-like interaction of direction-sensitive movement detectors, which become direction-insensitive at higher input frequencies.

4.2.4. Testing the Geometry of the Inhibition. In all previous experiments the ground texture covered essentially 360° of the visual field of the fly. In an additional series of experiments we have therefore tested how the inhibitory influence (at phase 0°) depends on the position and on the extension of the textured ground.

The first experiment is presented in Fig. 19. A black, 3° wide, vertically oriented stripe was oscillated around the positions $\psi_0 = \pm 30°$ with an amplitude of $\pm 1°$ and a frequency of 2.5 Hz. White screens, 12° wide, were mounted at the positions $\psi_0 = \pm 30°$ between the stripe and the ground. If the stripe is oscillated and the ground is at rest, the test-fly is attracted by the oscillating stripe; we define again the average value of this reaction as "standard". Figure 19 indicates how the response of the fly diminishes and even reverses sign when the angular extent of the oscillated random-dot textured ground is increased between $\gamma = 60°$ and $\gamma = 360°$. Oscillation amplitude and frequency are the same as for the stripe. The relative phase relation between stripe and ground is zero. The edges of the ground texture were covered with white screens. The front part of the panorama ($\gamma = 0°$ to $\gamma = 60°$) contained no texture but was white throughout the experiment. The experimental conditions are indicated in the inset of Fig. 19. The result shows that – under the conditions described here – the response of the fly decreases in proportion to the angular field covered by the ground texture, except for

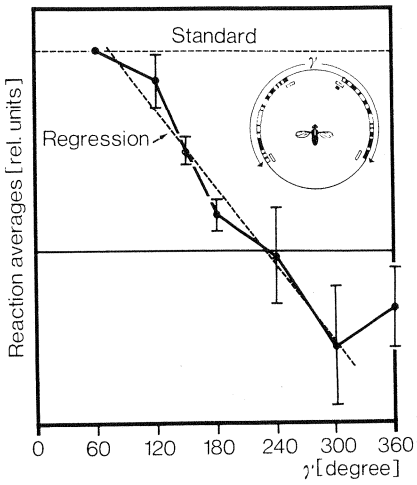

Fig. 19. Object-ground experiment testing the range of the fourth-order interactions. A black, 3° wide, vertically oriented stripe, extending over the lower half of the panorama, is oscillated at positions $\psi_0 = \pm 30°$ with an amplitude of $\pm 1°$ and a frequency of 2.5 Hz. Between oscillating stripe and resting or oscillating ground, 12° wide, stationary white screens are inserted to cover the front edges of the ground texture, as indicated in the inset. As in the experiments reported before, the ground consists of the same random-dot texture which covers part of the panorama from $\gamma = 60°$ to $\gamma = \gamma_{max} \leqq 360°$. A second pair of white screens, 12° wide, covers the back edges of the textured ground. Throughout the experiments the front part of the panorama, between $\gamma = 0°$ and $\gamma = 60°$, and the back part, between $\gamma = \gamma_{max}$ and 360° is white. The figure contains the time averages of the torque responses from 10 test-flies. The "standard" response refers to the condition that only the stripe was oscillated and the ground kept at rest. The individual points (and their standard deviations of the mean) indicate how the response depends on the area covered by the textured ground in the region $60° \leqq \gamma \leqq 360°$ when the ground is oscillated with the same amplitude and frequency as the stripe (relative phase is $\varphi = 0°$). The dotted line is a regression line for the mean values in the region $60° \leqq \gamma \leqq 300°$. Each point is an average from 10 individual flies. The vertical bars denote the error of the mean

the region between $\gamma = 300°$ and $\gamma = 360°$. Conversely, the strength of the inhibitory action is about in proportion to the angular region covered by the texture, at least in the range $60° < \gamma < 300°$. This finding is not in conflict with the hypothesis that the lateral inhibitory network is rather homogeneously distributed at least in the ψ-direction.

More surprising are the experimental results, shown in Fig. 20, which were obtained under slightly different conditions. As indicated in the inset of Fig. 20, also the front part ($0 \leqq \gamma < 60°$) was covered by the random-dot textured ground. Again, stripe and ground were oscillated with the same amplitude and frequency as in the preceeding experiment. The result, plotted in Fig. 20, indicates that with a larger angular extent of the ground, the response of the fly diminishes or conversely, the strength of the inhibitory influence increases. At $\gamma = 240°$, however, the response rises to

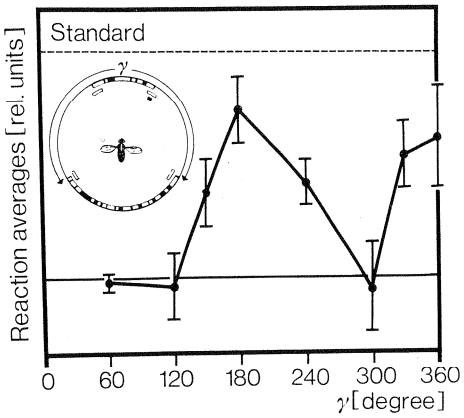

Fig. 20. Conditions as specified in the legend of Fig. 19. However, in the experiments reported here, the front part of the panorama between $\gamma=0°$ and $\gamma=60°$ is also covered by the random-dot textured ground. For further details see text

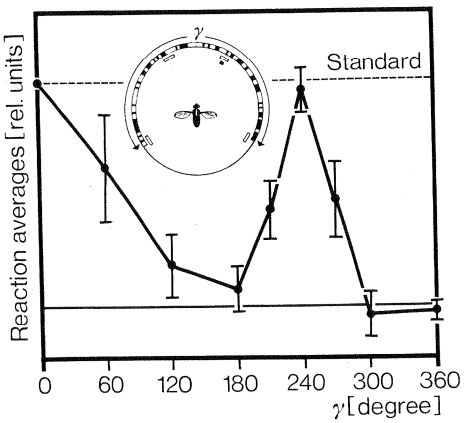

Fig. 21. Conditions as specified in the legend of Fig. 19. However, in the experiments reported here the front part of the panorama between $\gamma=0°$ and $\gamma=60°$ and part of the back part are covered by the random-dot textured ground. For $\gamma=60°$ as well as for $\gamma=360°$ only the front part is covered by the ground whereas for values between 60° and 360°, part of the ground is white and part of the ground is textured as indicated in the inset of the figure

about the "standard" value and then falls off to about zero at $\gamma=300°$. In other words, the strength of the inhibitory influence is reduced to about zero when the ground texture covers about 240° of the panorama and the object ist at $\psi_0=\pm 30°$. White screens 12° wide, are positioned between the stripe and the ground texture and cover the edges of the oscillating ground. The peak of the response, at $\gamma=240°$, is very sensitive to any changes of the texture in the front region. For example when a 20° wide screen is inserted in the front region, covering 20° of the textured ground, the response peak drops from about "standard" to 10% of the "standard" units. Consequently, the front parts of the two compound eyes – at least the region of their visual overlap – have a dramatic effect on the functional organization of the lateral inhibitory network. The details of this effect are not yet understood.

The peculiar influence of the front parts of the two compound eyes on the lateral interactions has been tested in another experiment, shown in Fig. 21. Here, the random-dot textured ground covered the front part (60°) and part of the back part (360 minus γ) of the eyes. Again, the effect of the front part is manifest if stripe (at positions $\psi_0=\pm 30°$) and ground are coherently ($\varphi=0°$) oscillated with the same amplitude ($\pm 1°$) and frequency 2.5 Hz. When the angular extension of the textured ground in the back part of the panorama is decreased, the time averaged response of the fly builds up and reaches about 0.75 standard units at $\gamma=180°$. It falls off to zero at $\gamma=300°$ and builds up again when $\gamma=360°$ is reached. The outcome of the experiment demonstrates again the decisive influence of the front parts of the two compound eyes and is consistent with the findings presented in Fig. 20.

Another experiment on similar lines suggests either that there may be wide angle interactions underlying figure-ground discrimination or that the corresponding network could have a recurrent structure. Figure 22 shows the experiment and its outcome. The response to coherent oscillation of figure and ground is of course zero. When the back part of the ground is eliminated (white screens cover the edges of the remaining front part) the attraction of the figure is quite significant although weaker than the standard attraction (stripe moving against the stationary background). If the front part of the ground texture is now eliminated, we measure a negative average response, i.e. a slight repulsion. Formally, we can summarize these results in the following way: let us call S the response due to the stripe and SF (SB) the response due to the interaction of the stripe with the front (back) part of the ground texture. Then the first experiment leads to $S+SF+SB=0$, whereas the sum of the responses in the successive two experiments is, formally, $S+SF+S+SB$. Since $S+SF+SB=0$, this sum should equal the standard response S. Figure 22 demonstrates, however, that this is not so and that the discrepancy is even significant. We are thus forced to postulate also an interaction term between front, back part and stripe (SFB). In this hypothesis the first equation becomes $S+SF+SB+SFB=0$ and there is no more inconsistency with the other two conditions. Such an interaction term (at least of degree 6 in our theoretical language) could arise from a recurrent structure of the inhibitory interactions. Another possibility is the following: if one of the two movement detectors is sensitive only to large field movement, its structure would probably consist of a sequence of small field movement detectors. Their summated output signals would then enter a nonlinear threshold. Such a

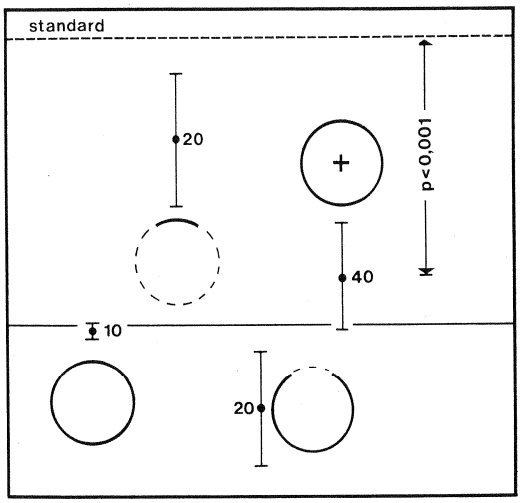

Fig. 22. A sequence of figure-ground experiments with different extensions of the textured ground. The figure consists of a black, 3° wide, vertically oriented stripe, extending over the lower half of the panorama and is oscillated at positions $\psi_0 = \pm 30°$ with an amplitude $\pm 1°$ and a frequency of 2.5 Hz. The oscillating ground is a random-dot texture of different extensions. The relative phase angle between figure and ground amounts to 0° throughout the experiment. The figure should be read from left to right. The result of the control experiment is shown on the left side. When the whole panorama is covered by the ground texture, the average response measured with 10 flies is zero. Next is the average response from 20 flies when the back part of textured ground is replaced by a white area. During the experiment white screens cover the edges of the remaining front part. The average response is below "standard". Next is plotted the average response from 20 flies when the front part of the ground is white and the back part random-dot textured. Again the edges of the textured ground are covered by white screens. Next we have plotted the sum of the last two experiments which is significantly different from the "standard" response. A "standard" response is elicited when only the figure oscillates and the ground is kept stationary. The vertical bars denote standard deviations of the means. For more details see text

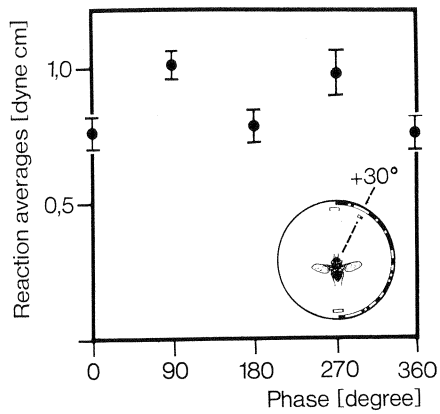

Fig. 23. Phase dependence of the figure-ground discrimination effect under monocular stimulation, as indicated in the inset. The figure consisted of a 6° wide, random-dot textured stripe which is oscillated around the mean positions $\psi_0 = \pm 30°$. The random-dot textured ground covered either 180° of the right or left half of the panorama. The edges of the textured ground were covered by white stationary screens each 9° wide. The oscillation frequency of figure and ground amounted to 2.5 Hz and the oscillation amplitude to $\pm 3°$. The solid points are averages from 15 flies. Each measurement lasted 2 min. The vertical bars denote standard errors of the mean. The experiment was carried out in the set-up described in Fig. 2a

scheme, for which low frequency experiments provide evidence, leads directly to interaction terms of the SFB type (see Part II).

It is important to mention a further point. In this paper we did not analyze the figure ground effect as a function of the object position in the vertical coordinate. Earlier experiments have shown that the effect is mainly present in the lower part of the eyes, below the equator, as it is the case for the position computation (Poggio and Reichardt, 1976; Heimburger et al., 1976). There are however, indications that figure-ground discrimination may be to some extent performed also in the upper part of the compound eye, although possibly with a different algorithm (see graph a in Table 5) which is also found in walking *Drosophila* (Bülthoff et al., in preparation).

4.2.5. Is Figure-Ground Discrimination a Binocular Effect? So far we have made the implicit assumption that figure-ground discrimination relies on local interactions, possibly of large angular extent. It is, however, conceivable that the effect requires binocular stimulation of the two eyes. However, this is not the case. Firstly, Virsik and Reichardt (1974) have demonstrated in closed-loop experiments, that the effect does not depend on relative depth between figure and ground. Secondly, Pick (1974b) uncovered the existence of fourth-order inhibitory interactions through monocular stimulations. Although it has not been conclusively proved, these interactions are probably identical with the graph *b* in Table 5 which underly figure-ground discrimination (see Poggio and Reichardt, 1976 and Part II).

In any case the experiment shown in Fig. 23 shows that, except for an additional constant (see Chap. 4.2.7), the phase dependency of the figure-ground discrimination effect remains unchanged under monocular stimulation. It can therefore be concluded that figure-ground discrimination is not strictly a binocular phenomenon.

4.2.6. The Range of the Inhibitory Interaction. An important question evidently concerns the angular range of the inhibitory interactions (see graphs of Table 5). Previous experiments (Pick, 1974b; Reichardt, 1978) have shown that lateral fourth-order inhibitory interactions affecting the position computation exist with an angular range between 6° and at least 20° (in the frontal part of the eye). This would mean that the angular distance between interacting

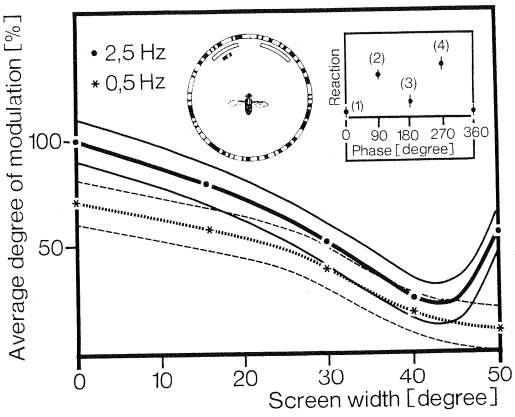

Fig. 24. Figure-ground phase experiments to test the range of interactions between a random-dot textured figure and a random-dot textured ground. White screens are mounted between the oscillating figure and the oscillating ground. The experimental parameter of each set is the angular width of the screens (see inset at the upper left). The 6° wide figure is oscillated around the mean positions $\psi_0 = \pm 30°$. The oscillating amplitudes of figure and ground amounted to $\pm 3°$. Phase portraits were measured at two different frequencies: 2.5 and 0.5 Hz. A typical portrait (at 2.5 Hz) is shown in the inset at the upper right. The "modulation" of the time averaged reaction declines with an increasing width of the screens, indicating the diminishing influence of the ground. The average "modulation", $\bar{m}$, defined by

$$\bar{m} = \frac{\frac{2\times(2)}{(1)+(2)} - 1 + \frac{2\times(4)}{(3)+(4)} - 1}{2}$$

(see inset at the upper right) is plotted as a function of the angular width of the white screens. The points ● represent measurements at 2.5 Hz and the crosses * measurements at 0.5 Hz. The areas around the two curves designate error regions. The results show that, for both frequencies (2.5 Hz; 0.5 Hz) the averaged "modulation" $\bar{m}$ decreases with increasing screen width, except for the 50° screens when only 10° of the front region of the random-dot textured ground is uncovered

movement detectors is no less than 6°. The fly's eye is therefore organized with an (nonlinear) excitatory center and inhibitory surround; this explains the findings reported in Sect. 4.2.1 where the discrimination effect was tested with different oscillation amplitudes of figure and ground.

In a series of experiments, we investigated how figure-ground discrimination depends on the width of a white screen inserted between the oscillating figure and the oscillating ground. The experiments were carried out in the mechanical device described in Fig. 2a. Figure and ground consisted of random-dot textures with contrast elements of 3° width. The angular width of the textured stripe amounted to 6°. Figure and ground were oscillated with an amplitude of $\pm 3°$. The mean positions of the figure were $\psi_0 = \pm 30°$. The tests were carried out at two differing oscillation frequencies at 2.5 and 0.5 Hz (see inset in Fig. 24). The qualitative phase portrait of the response does not depend significantly on the screen's width and reflects closely the one of Figs. 6 and 18 at high and low frequencies respectively. The phase dependence of the time averaged responses declines when the width of the screens is increased. A proper definition of "modulation" is given in the legend of Fig. 24. The two curves in Fig. 24 represent the dependence of the "modulation" on the increasing width of the screens. Thus, the effect of the inhibitory interaction is still present over a range of almost $\pm 20°$. In addition, the decrease of the effect with increasing screen width is about the same at both high and low oscillation frequencies. This result supports the hypothesis that the frequency dependence of the phase portrait is a property of one interacting nerve net and does not depend on two different nets, one responding mainly at 2.5 Hz and the other at 0.5 Hz oscillation frequencies. In this second case, one may expect the geometry of such nets to be different, in particular with a different range for inhibition.

4.2.7. How are the Excitatory and Inhibitory Contributions Balanced? The conclusions we have drawn from the figure-ground experiments are not in conflict with the hypothesis that the "excitatory" contributions from the position computations [k_0 in Eq. (1)], are cancelled rather locally by the fourth-order relative movement computations [k_4 in Eq. (1)] when there is no relative motion between figure and ground. One would expect, however, that the relative balance of excitation and inhibition would depend on various parameters, like the contrast of the pattern and its spatial frequency content. In terms of the model we suggest it would be indeed odd if excitation would be exactly cancelled by inhibition over a broad parameter range.

The problem can be made more precise by the following argument: If $E_R(E_L)$ designates the amount of excitatory contributions provided by the right (left) eye and $I_R(I_L)$ the amount of inhibitory contributions provided by the right (left) eye, the reaction of a fly for given stimulus configuration is

$$\bar{R} \sim (E_R - I_R) - (E_L - I_L) \qquad (3)$$

since excitations (inhibitions) stimulated from the right eye result in a positive (negative) torque whereas excitations (inhibitions) from the left eye lead to a negative (positive) torque response. When figure and ground (consisting of the same texture) are oscillated coherently all around the fly, $E_R = E_L$, $I_R = I_L$ and $\bar{R} = 0$. From the experiments reported in this paper, it can not be concluded that $E_R = I_R$ and $E_L = I_L$. The only conclusion we can draw, is $E_R = aI_R$ and $E_L = aI_L$, with "a" as an undetermined positive parameter. This parameter can be inferred from an experiment where only one of the two compound eyes is stimulated by a

180° wide textured ground with boundaries at $\psi_0 = 0°$ and $\psi_0 = \pm 180°$. The edges are covered by white screens and the ground is oscillated with 2.5 Hz and an amplitude of $\pm 1°$. From a sequence of such experiments we conclude that the flies are attracted by the oscillating (half) ground with a strength of 0.65 ± 0.07 dyne × cm. The outcome of these experiments leads to a value of "*a*" (under these conditions) larger than 1. Consequently, overall excitation elicited in one of the two compound eyes overrides the inhibition elicited in the same eye. The other figure-ground experiments reported in this paper are differential experiments, expressing the difference of excitatory and inhibitory contributions from the two compound eyes, one stimulated only by the ground texture, the other stimulated by the figure and the ground.

4.2.8. Are Stationary Figures Attractive when the Ground is Oscillated? Another important point in the analysis of the figure-ground discrimination is the assumption that – as in the case of position computation – stationary images on the retina, irrespective of their brightness, have no influence on the behavioural response. If this is so, the interactions involved in this computation would only operate on time dependent signals. In order to test this assumption, a sequence of experiments was undertaken with stationary stripes (16° to 24° angular width) whose surface were either black, white or a random-dot texture. The ground always consisted of a random-dot texture which was oscillated with a frequency of 2.5 Hz and an oscillation amplitude of $\pm 1.4°$. The results of these experiments are plotted in Fig. 25. Let us first consider the associated three control experiments. The open circles represent reaction averages to in-phase oscillations of ground and random-dot textured stripes. These averaged responses are zero. When only a random-dot textured stripe is oscillated with an amplitude of $\pm 1.4°$ and the ground is at rest, the averaged response (filled circles) increases with increasing stripe width. The same results are obtained when figure and ground are oscillated with equal amplitudes, but differing frequencies (2.5 Hz for the stripe and 1.8 Hz for the ground). As we have discussed before, under these conditions the mutual inhibitory interactions do not contribute to the response and the effect of the stripe (figure) is "independent" from the ground. In the other experiments the stripe (figure) was at rest in front of the ground texture and only the ground was oscillated. The fact that these reaction averages are essentially zero (with only one exception at 24° stripe width) and independent of texture and brightness of the stripe is in accordance with the hypothesis that only brightness changes that result from motions or from flicker can influence the figure-ground computations.

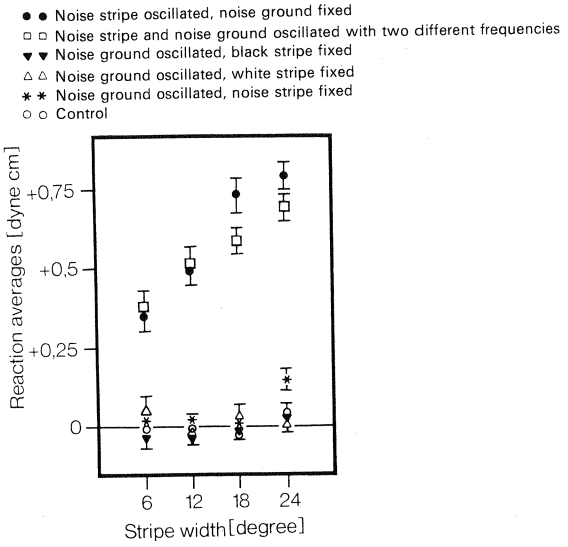

Fig. 25. Reaction averages to oscillating or stationary figures (vertically oriented stripes of different width) and/or a stationary or oscillating random-dot textured ground. The experiments were carried out as described in the legend of Fig. 2a. The stripes (figures) when oscillated, were positioned in the mean at $\psi_0 = \pm 30°$. The oscillation frequency amounted to 2.5 Hz and in the case of the two frequencies experiment 2.5 Hz for the figure and 1.8 Hz for the ground. Oscillation amplitudes were $\pm 1.4°$. Each point is the reaction average from 10 flies. The vertical bars denote the standard errors of the mean. The different symbols refer to the following experimental conditions. ○ Control (random-dot textured ground and random-dot textured figure are oscillated in phase). ● Random-dot textured figure is oscillated, random-dot textured ground kept stationary. □ Random-dot textured figure and ground are oscillated with two different frequencies. ▼ Random-dot textured ground is oscillated, black figure is kept stationary. ▽ Random-dot textured ground is oscillated, white figure is kept stationary. ✱ Random-dot textured ground is oscillated, random-dot textured figure is kept stationary. For further explanation see text

It is important to observe that these findings suggest that around the $\psi_0 = \pm 30°$ regions excitatory and inhibitory contributions cancel each other. Otherwise the average response to a stationary stripe should have been expected to be negative (fly repelled by the stripe) because of a larger contribution from the other eye. Since in the previous section we have concluded that the overall excitation from one eye is larger than the corresponding inhibition, we are forced to conclude that excitatory and inhibitory contributions are inhomogeneously distributed in the eye (at least in ψ-direction). On the other hand, the computer experiments of Part II show that the effect of a stationary object in front of moving texture depends strongly on various parameters (frequency, texture, etc.). Other experiments have confirmed this, showing that the results of this section can not be easily extrapolated to situations characterized by different parameters (compare also the computer experiments of Part II). Of course, saturation effects on each eye's

output cannot be fully excluded as an alternative explanation.

5. Discussion

The basic picture emerging from the experiments described in this paper implies that the algorithm used by the fly's visual system to detect an object moving relative to a textured ground has a rather simple structure. The algorithm can be described in terms of multiplication-like interactions between direction-sensitive movement detectors, which become direction-insensitive at higher input frequencies. The computer implementation described in Part II, illustrates alternative descriptions of this algorithm. Consider an array of direction-sensitive movement detectors: then the algorithm implemented by the fly at low oscillation frequencies roughly corresponds to the rule: an object exists where there is a discontinuity in the sign of detector outputs. At higher oscillation frequencies the rule would be: an object exists where there is (for some time) a small area of activity in the detector array, while everywhere else the detectors are silent. These two simple rules represent the basic qualitative properties of the fly's behaviour in our experiments.

In this paper we have stressed the discrimination of relative movement as the basic property of an algorithm used by the fly. It is clear, however, that interactions of the type described measure not only coherence of movement but also "coherence" of spatial texture. In fact, when the figure's spatial spectrum is very different from the ground's spectrum, the fourth-order inhibitory interactions may lead to a rather weak contribution and consequently to a discrimination of the figure even in the case of coherent motion. This can occur because movement detectors, on which the relative movement algorithm is based, deliver a signal that depends not only on the velocity of a visual pattern, but also on its spatial spectrum, especially when it has symmetry (i.e. direction-insensitive) properties (see Part II). Thus lateral nonlinear fourth-order interactions play an important role in determining the attractiveness of a complex pattern (see Poggio and Reichardt, 1976). Potentially, the fourth-order interactions represent a mechanism computing position-dependent information from more than one photoreceptor input, in addition to the one-input flicker detectors described by Pick (1974a). The presence of the fourth-order system has profound effects also for spatially localized objects without a ground texture. For instance, a contrasted stripe wider than about 6° is more attractive when oscillating than when flickered, because in the latter case the fourth-order interactions inhibit the flicker detectors. Because of this, a moving stimulus is usually more effective than a flickered one (see Part II for a detailed discussion).

In a more general perspective, the ethological significance of the experiments described here is not completely clear. Flies, as other insects, certainly need to discriminate small objects moving relative to the environment. Presently, however, we don't know of a free flight behaviour that is certainly based on this algorithm for relative movement.

In this context it is interesting to mention that figure-ground discrimination is not confined to open-loop experiments. It has been observed under closed-loop conditions as well (Virsik and Reichardt, 1976), supporting the central thesis of the phenomenological theory (Reichardt and Poggio, 1976) which maintains that closed-loop orientation behaviour can be quantitatively predicted from a knowledge of the open-loop responses of the fly. Thus, the reafference principle (Mittelstaedt, 1971) is not necessarily required, at least in the behaviour studied here. An insect can easily discriminate self-movement from object movement by the relative movement algorithm we have discussed, without need of reafferent information. Our data show that figure-ground discrimination is not a strict closed-loop phenomenon, as one would expect if reafferent mechanisms were present. This point is analogous to Palka's (1972) conclusion, based on physiological experiments. Thus, a likely function of the relative movement algorithm is to discriminate self-motion from object-motion, a task which may be difficult to perform otherwise for a flying insect.

Detection of relative movement may be considered as a first step in using information contained in the optical flow field. Relative motion cues often lead to a dissection of the environment into separate "objects", each one moving as a "coherent" entity. These cues can also be provided by motion of the fly, as a result of parallax effects. The algorithm analyzed in this paper can underly such a dissection of the visual environment. Again, it is too early to specify the role of the relative movement algorithm in the behaviour of the fly. Is it only used to detect moving targets? Does it perhaps play a more sophisticated role in separating various objects in the environment? Several other possibilities are conceivable. For instance, the interactions studied here may also be involved in measuring the contraction and expansion of a pattern, a computation of obvious usefulness which was not explored in this paper.

An important question at a different level concerns the neural circuitry that implements the algorithm analyzed in this paper. The problem depends strongly, of course, on the actual circuitry underlying direction-selectivity (to motion) of nerve cells. A specific synaptic interaction has been recently proposed as a physiological mechanism responsible for direction-selectivity (Torre and Poggio, 1978). Similar synaptic interactions

may form the basis of dendritic local circuits that subserve the nonlinear fourth-order interactions. Of course, several other schemes, based for instance on threshold properties of neurons are likely candidates. Unfortunately, very little can be said about even the location in the fly's visual pathway of the neural counterpart of the relative movement computation. It is furthermore unclear whether the nonlinear interactions are recurrent (compare Poggio and Reichardt, 1976).

An additional question that we are presently studying concerns the dynamics of the relative movement response and the relationship of its onset with the progressive-regressive phase of figure and ground motion. It is for instance conceivable that most of the response takes place during such phases in which the figure moves progressively (from front to back) and simultaneously the ground stays or moves regressively on the same eye. The dependence of figure-ground discrimination on the contrast structure of the figure is also an issue that deserves future studies. It may help to establish connections with "on" and "off" properties of underlying neural mechanisms. Problems of this type are clearly important for finding out how the algorithm characterized in Table 4 is realized by the nervous system of the fly.

Palka (1969) has shown in crickets that large and whole field stimuli evoke mainly inhibition in the lobular giant movement detector system, a result corroborated by O'Shea and Fraser-Rowell (1975). Habituation is rapid in response to repeated small visual field movements, but (prolonged) whole field movements do not reduce the responsiveness of the movement detector neurons to subsequent small field movements. O'Shea and Fraser-Rowell have also demonstrated that protection from habituation is achieved by lateral inhibition which acts prior to the site of response decrement to suppress the response to whole field stimuli. Their work suggests that there are two separate inhibitory mechanisms in the locust, suppressing the response to large field movements. A first mechanism is active for rapid movements of the field, a second mechanism seems to be graded in proportion to the proximity of the large stimulating field to a small target. The dependence on spatial separation is typical of a lateral inhibitory network. It is tempting to compare these mechanisms with the two different relative movement algorithms found in the fly for low and high frequencies of oscillation, respectively. The experimental data plotted in Fig. 24, however, provide evidence against such a simple interpretation. In addition, the stimulus situation used in the physiological experiments are not easily comparable with ours. The difficulty of a comparison also arises for several other experimental situations, for instance in psychophysics and vertebrate physiology, that bear some similarities with our data. In Part II we will discuss this matter in more detail.

Finally we would like to stress that the overall visual control of flight in flies relies on a number of other algorithms, for instance the algorithms underlying landing or distance evaluation (see Reichardt and Poggio, 1980). The central role of movement detection in the relative movement algorithm also suggests that several of these algorithms (which have still to be characterized) may be based on computations performed on the movement field, as measured by elementary movement detectors distributed everywhere in the eye. After all, the structure of the optical flow is full of useful information, especially for a flying animal and it would indeed be surprising if insects do not make extensive use of it. The field of image velocities on the retina contains, for example, information about the slant of surface elements of objects and about the motion of the fly itself. Rather simple operations on the output of an array of movement detectors could provide to a flying fly rough information about the three-dimensional structure of the world.

Acknowledgments. We would like to thank H. Bülthoff, K. Hausen, D. Marr, C. Wehrhahn, and especially J.D. Cowan for many critical discussions and useful suggestions. J.D. Cowan also corrected the English. We are grateful to Mrs. I. Geiss for typing the manuscript and L. Heimburger for skilled experimental assistance and for drawing the figures and tables.

References

Buchner, E.: Bewegungsperzeption in einem visuellen System mit gerastertem Eingang. Dissertation Eberhard-Karls-Universität Tübingen, 1974

Bülthoff, H., Poggio, T., Reichardt, W.: Figure-ground discrimination by relative movement in the visual system of the fly. Part II: Movement and relative movement algorithms. To be submitted to Biol. Cybernetics (1980)

Eckert, H.: Optomotorische Untersuchungen am visuellen System der Stubenfliege *Musca domestica* L. Kybernetik **14**, 1–23 (1973)

Fermi, G., Reichardt, W.: Optomotorische Reaktionen der Fliege *Musca domestica.* Kybernetik **2**, 15–28 (1963)

Götz, K.G.: Optomotorische Untersuchungen des visuellen Systems einiger Augenmutanten der Fruchtfliegen *Drosophila.* Kybernetik **2**, 77–92 (1964)

Götz, K.G.: Principles of optomotor reactions in insects. Bibl. Ophthal. **82**, 251–259 (1972)

Hassenstein, B.: Ommatidienraster und afferente Bewegungsintegration (Versuche am Rüsselkäfer *Chlorophanus viridis*). Z. Vgl. Physiol. **33**, 301–326 (1951)

Hassenstein, B.: Über die Wahrnehmung der Bewegung von Figuren und unregelmäßigen Helligkeitsmustern. Z. Vgl. Physiol. **40**, 556–592 (1958)

Hassenstein, B.: Optokinetische Wirksamkeit bewegter periodischer Muster. Z. Naturforsch., Teil B **14**, 659–674 (1959)

Hassenstein, B., Reichardt, W.: Reihenfolgen-Vorzeichenauswertung bei der Bewegungsperzeption des Rüsselkäfers *Chlorophanus.* Z. Naturforsch., Teil B **11**, 513–524 (1956)

Heimburger, L., Poggio, T., Reichardt, W.: A special class of nonlinear interactions in the visual system of the fly. Biol. Cybernetics **21**, 103–105 (1976)

Hengstenberg, R., Götz, K.G.: Der Einfluß des Schirmpigmentgehalts auf die Helligkeits- und Kontrastwahrnehmung von *Drosophila*-Augenmutanten. Kybernetik **3**, 276–285 (1967)

Julesz, B.: Experiments in the visual perception of texture. Sci. Am. **232**, 34–43 (1975)

McCann, G.D., MacGinitie, G.F.: Optomotor response studies of insect vision. Proc. R. Soc. London, Ser. B **163**, 369–401 (1965)

Marmarelis, P., McCann, G.D.: Development and application of white-noise modelling techniques for studies of insect visual nervous system. Kybernetik **12**, 74–90 (1973)

Mittelstaedt, H.: Reafferenzprinzip, Analogie und Kritik. Vorträge der Erlanger Physiologentagung 1970. Keidel, W.D., Plattig, K.H. (eds.). Berlin, Heidelberg, New York: Springer 1971

O'Shea, M., Fraser-Rowell, C.H.: Protection from habituation by lateral inhibition. Nature **254**, 53–54 (1975)

Palka, J.: Moving movement detectors. Am. Zool. **12**, 497–505 (1972)

Palka, J.: Discrimination between movements of eye and object by visual interneurons of crickets. J. Exp. Biol. **50**, 723–732 (1969)

Pick, B.: Visual flicker induces orientation behavior in the fly *Musca*. Z. Naturforsch., Teil C **29**, 310–312 (1974a)

Pick, B.: Das stationäre Orientierungsverhalten der Fliege *Musca*. Dissertation, Eberhard-Karls-Universität Tübingen, 1974b

Pick, B.: Visual pattern discrimination as an element of the fly's orientation behaviour. Biol. Cybernetics **23**, 171–180 (1976)

Pick, B., Buchner, E.: Visual movement detection under light- and dark-adaptation in the fly *Musca domestica*. J. Comp. Physiol. (in press, 1979)

Poggio, T.: Processing of visual information in flies: from a phenological model towards the nervous mechanisms. In: Atti della prima riunione Scientifica (Camogli, 1973). Soc. Ital. Biofis. Pura e Applicata, pp. 217–225, 1974

Poggio, T., Reichardt, W.: Considerations on models of movement detection. Kybernetik **13**, 223–227 (1973a)

Poggio, T., Reichardt, W.: A theory of the pattern induced flight orientation of the fly *Musca domestica*. Kybernetik **12**, 185–203 (1973b)

Poggio, T., Reichardt, W.: Visual control of orientation behaviour in the fly. Q. Rev. Biophys. **9**, 377–438 (1976)

Poggio, T., Reichardt, W.: Characterization of nonlinear interactions in the fly's visual system. In: Recent theoretical developments in neurobiology. Neurosciences Research Program bulletin. Cambridge, Mass.: MIT Press (in press) 1980

Poggio, T., Reichardt, W.: Properties of polynomial algorithms multi-input systems. To be submitted to Biol. Cybernetics (1980)

Reichardt, W.: Autokorrelations-Auswertung als Funktionsprinzip des Zentralnervensystems (bei der optischen Wahrnehmung eines Insektes). Z. Naturforsch. **12b**, 488–457 (1957)

Reichardt, W.: Autocorrelation; a principle for the evaluation of sensory information by the central nervous system. In: Sensory Communication. Rosenblith, W.A. (ed.), pp. 303–318. New York: John Wiley 1961

Reichardt, W.: Movement perception insects. In: Processing of optical data by organisms and machines. Reichardt, W. (ed.), pp. 465–493. London, New York: Academic Press 1969

Reichardt, W.: The insect eye as a model for analysis of uptake, transduction, and processing of optical data in the nervous system. In: The Neurosciences, second study program. Schmitt, F.O. (ed.), pp. 494–511. New York: Rockefeller Univ. Press 1970

Reichardt, W.: Musterinduzierte Flugorientierung. Verhaltens-Versuche an der Fliege *Musca domestica*. Naturwissenschaften **60**, 122–138 (1973)

Reichardt, W.: Interactions in the visual system. In: Proceedings of the first symposium on testing and identification of nonlinear systems. McCann, G.D., Marmarelis, P.Z. (Eds.), pp. 174–190. California Institute of Technology Pasadena, California, March 17–20, 1975

Reichardt, W.: Figure-ground discrimination by the visual system of the fly. In: Lecture notes in biomathematics, Vol. 21: Theoretical approaches to complex systems. Proceedings, Tübingen 1977. Heim, R., Palm, G. (ed.), pp. 117–146. Berlin, Heidelberg, New York: Springer 1978

Reichardt, W., Poggio, T.: Visual control of orientation behaviour in the fly, Part I. A quantitative analysis. Q. Rev. Biophys. **9**, 3, 311–375 (1976)

Reichardt, W., Poggio, T.: Visual control of flight in flies. In: Recent theoretical developments in neurobiology. Neuroscience Research Program. Cambridge, Mass. MIT Press (in press) 1980

Reichardt, W., Varjú, D.: Übertragungseigenschaften im Auswertesystem für das Bewegungssehen. Z. Naturforsch., Teil B **14**, 674–689 (1959)

Reichardt, W., Wenking, H.: Optical detection and fixation of objects by fixed flying flies. Naturwissenschaften **56**, 424–425 (1969)

Thorson, J.: Small-signal analysis of a visual reflex in the locust. I. Input parameters. Kybernetik **3**, 41–53 (1966a)

Thorson, J.: Small-signal analysis of a visual reflex in the locust. II. Frequency dependence. Kybernetik **3**, 53–66 (1966b)

Torre, V., Poggio, T.: A synaptic mechanism possibly underlying directional selectivity to motion. Proc. R. Soc. London, Ser. B **202**, 409–416 (1978)

Varjú, D.: Optomotorische Reaktionen die auf Bewegung periodischer Helligkeitsmuster. Z. Naturforsch., Teil B **14**, 724–735 (1959)

Varjú, D., Reichardt, W.: Übertragungseigenschaften im Auswertesystem für das Bewegungssehen. II. Z. Naturforsch., Teil B **22**, 1343–1351 (1967)

Virsik, R., Reichardt, W.: Tracking of moving objects by the fly *Musca domestica*. Naturwissenschaften **61**, 132–133 (1974)

Virsik, R., Reichardt, W.: Detection and tracking of moving objects by the fly *Musca domestica*. Biol. Cybernetics **23**, 83–98 (1976)

Wehrhahn, C.: Verhaltensstudie zur musterorientierten Höhenorientierung der Fliege *Musca domestica*. Dissertation, Eberhard-Karls-Universität Tübingen, 1974

Wehrhahn, C., Reichardt, W.: Visually induced height orientation of the fly *Musca domestica*. Biol. Cybernetics **20**, 37–50 (1975)

Received: July 26, 1979

Prof. Dr. W. Reichardt
Max-Planck-Institut
für biologische Kybernetik
Spemannstraße 38
D-7400 Tübingen
Federal Republic of Germany